PRELIMINARY DESIGN OF A JOINED WING HALE UAV

D. Verstraete, M. Coatanea , P. Hendrick
Université Libre de Bruxelles, Laboratory of AeroThermoMechanics

Keywords: *HALE UAV, preliminary design, joined-wing*

Abstract

High Altitude Long Endurance Unmanned Aerial Vehicles (HALE UAVs) could provide an improved service and/or flexibility at a reduced cost over existing systems for a vast number of civil patrol and surveillance applications.

However, at current state of the technology, the design of HALE UAVs requires innovative solutions for both the aircraft configuration as well as the propulsion system. As a lower propulsive power as well as a light wing structural weight is key drivers in the design of the UAV, a joined wing potentially offers excellent synergies for this design. After all, joining the tips of the two sections of the wing significantly reduces the induced drag as well as the structural weight of the wing.

This paper presents the preliminary design of a joined wing HALE UAV for an endurance of one month at summer solstice. The estimation of the take-off and empty mass as well as the aerodynamic characteristics of the UAV are given as well as a detailed motivation of the selected mission specification.

1 Introduction

HALE UAVs could provide an improved service and/or flexibility over existing systems for a vast number of civil applications, ranging from border patrol and coastal surveillance over monitoring of natural disasters, meteorology and cartography to highly flexible telecommunication relay stations. Airborne platforms that remain aloft for weeks to months at altitudes between 15 and 22 km namely provide an advantage over satellite systems in terms of reduced costs, increased flexibility and higher precision.

Seen the wide range of applications for this type of airplane, numerous studies have been executed in the near past after successful flights of Pathfinder, Helios, Global Hawk and Global Observer. The Shampo vehicle (ref. [7] and [8]) as part the HELIPLAT program (FP V of the European Commission), the European COST action 297, HAPCOS, funded by the European Science Foundation (ref. [15]), the Pegasus platform developed by Verhaert Space and Qinetiq (ref. [2] and [3]) and the Sun-H2 project funded by the Walloon Region in Belgium (ref. [14]) are only a few of the numerous examples that could be cited here.

However, at the current state of technology, the design of HALE UAVs poses many challenges and requires innovative solutions for both the aircraft configuration as well as the propulsion and energy storage systems. To enable a flight endurance in the order of weeks, the propulsion system needs to be able to provide the power for the flight day and night, which leads to a very heavy fuel load when using a non-regenerative system. If a regenerative system is used however, the power train needs to be doubled. One system is needed for the daytime and a second one provides the power for the flight throughout the night. As a consequence of this unavoidable redundancy, a low propulsive power is a key driver in the design. This entails the need for a low UAV weight and a low flight speed. As such, low Reynolds number aerodynamics becomes an issue in the design too.

The first section of the paper describes the de-

sign mission specifications. Then the selection of the configuration of the HALE UAV is detailed. Both the power and energy storage system as well as the aircraft configuration are treated. Once the selection is made the power and energy storage system are sized, before going into more detailed calculations of the aircraft characteristics. The take-off mass, wing area and power required are determined as well as the aerodynamic characteristics of the wing.

2 Design Mission Specifications

The mission specifications for the design under consideration are very critical. Selecting low values for parameters as endurance and payload mass and power will lead to a UAV that is only able to fly a limited amount of different missions. Too optimistic values will on the other hand lead to a too challenging and potentially even unfeasible design at current technology. The selected values for the mission specifications are given in Table 1.

Table 1 Mission Specifications

Payload	
Mass	50 kg
Volume	0.5 m^3
Power	2 kW
Performance	
Endurance	1 month
Cruise Altitude	15-22 km
Latitude	40 °N
Cruise Speed	20-40 m/s

As shown in the table, a payload mass of 50 kg is considered, which lies in the lower range of payload masses for UAVs suited for the civil and commercial market (20 - 750 kg, ref. [11]). The mass, volume and power for the payload are selected to allow the installation of a SAR with a resolution of about 1 m or an optical/IR sensor with a resolution of about 0.1 m (ref. [13]).

As the main envisaged applications for this HALE UAV are forest fire monitoring and the use as an airborne communication relay station, an endurance of one month at summer solstice at 40° Northern Latitude was selected. This gives the UAV a reasonable flexibility in terms of operation without being overly demanding. In periods with a lower sunlight intensity, a mission of about one month would nonetheless still be possible if the payload mass and power required would be reduced. However, this will probably require the use of a new, expensive sensor developed specifically for this application. This approach was for instance taken in the Pegasus project to reduce the overall aircraft mass (ref. [3]).

The cruise altitude is chosen between 15 and 22 km for several reasons. First of all, it places the aircraft well above the civil aviation airspace, leading to an easier operation of the UAV and presumably also an easier certification. After all, integration of UAVs into the traffic-controlled airspace is still a critical issue hindering the certification of any type of UAV (ref. [11]). A high cruising altitude furthermore leads to a wider area coverage. At 10 km altitude, the horizon is situated at about 250 km while at 20 km altitude the horizon lies at 500 km from the aircraft (ref. [4]). From 17 km altitude, an area of about 300 km diameter would be covered for communication transmission with the proper irradiation diagram for the onboard antenna (ref. [7]).

The main reason for adopting the chosen cruise altitude is all things considered the occurrence of lower mean wind speeds. As shown on Figure 1, a low wind speed can be found between 15 and 25 km altitude. The ceiling was nonetheless set to 20 km to keep the aircraft size and wing area within reasonable limits. During the night phase, a glide down to 17 km is permitted to reduce the amount of energy needed for the night-time propulsion. After all during the glide phase, only the power of the payload and avionics needs to be provided which could significantly reduce the size and mass of the energy storage system required for the night-time flight phase.

3 Configuration selection

Below, first the choice of the type of propulsion and energy storage system is elucidated. Then

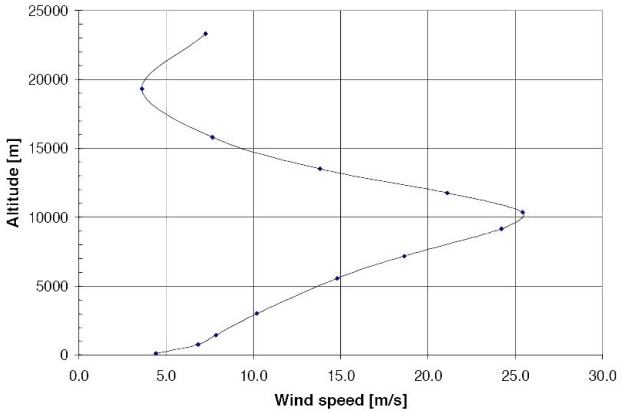

Fig. 1 Mean wind speeds over Belgium (ref. [3])

the reasons for selecting a joined wing are given.

3.1 Propulsion and energy storage systems

Principally, several types of propulsion system would be feasible for the UAV, ranging from a classical piston engine based propulsion system to a system based on solar energy and an energy storage system for the night flight,... Seen the relatively high endurance, using only a non-regenerative propulsion systems can be ruled out with currently available technology. Even when using hydrogen as a fuel, an excessively high fuel mass would namely be needed to obtain an endurance of 1 month. Therefore, only a system based on solar energy will be considered.

The main disadvantage of a solar panel based system is the need for a double power generating system. During the day, the energy derived from the solar panels is used to propel the UAV. At night, however, an additional system is required. This night-time system could consist out of batteries or a regenerative fuel cell/electrolyser. Relying on the energy from the sun furthermore makes the power available during the day dependent on both the time of the year for the mission as well as the latitude and altitude of the foreseen flights. This could lead to a reduced operational flexibility.

3.2 Joined Wings

One of the prime drivers in the design of a HALE UAV is the minimization of the power required during the flight. A low cruise speed therefore needs to be adopted. As a low speed, high altitude flight is envisaged a large wing area is needed. To reduce the induced drag, a high aspect ratio furthermore needs to be adopted. Seen the importance of these drivers, a joined wing was considered in this study.

Due to the reduction of the strength of the tip vortices, a joined wing configuration leads after all to a very low induced drag. As was shown by Wolkovitch in ref. [12], a significant increase in the wing Oswald efficiency factor can be obtained with a joined-wing. Wolkovitch shows that a span efficiency factor as high as 1.4 or 1.5 could be obtained with the proper vertical separation of the wing, as shown on Figure 2.

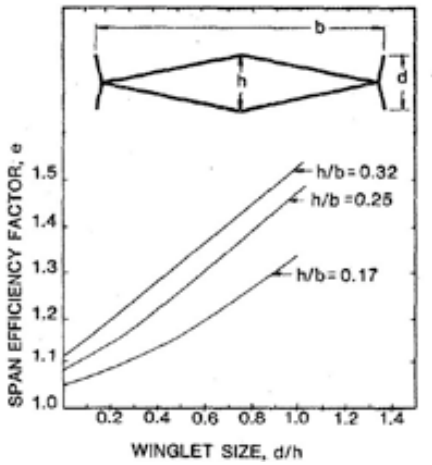

Fig. 2 Joined wing Oswald efficiency factor (ref. [12])

Besides the significant reduction in induced drag, a joined wing configuration also leads to a low structural wing weight due to the high stiffness in both bending and torsion of the closed box that is formed by joining the two sections of the wing. This is particularly attractive for this applicaton seen the relative importance of the wing weight in the overal weight build-up of the aircraft. According to ref. [12], a joined wing furthermore leads to a high maximum lift coefficient and a low wetted surface area, which reduces the

parasite drag of the aircraft.

For a solar powered HALE UAV application, both sections of the wing need to be swept so that the upper wing does not block the direct radiation of the sun falling on the lower wing. As such, the wing structural weight slightly increases and the efficiency of the control surfaces is reduced.

4 Propulsion system and energy storage system dimensioning

During the day, the solar panels need to provide the energy for the avionics and payload, for the propulsion of the UAV and to recharge the energy storage system, which can consist out of rechargeable batteries or a regenerative fuel cell with hydrogen, oxygen and water tanks. Fig. 3 shows a block sketch of the propulsion and energy storage system. Below, first the power required from the energy system during the day and the night will be determined. Then the different components of the system will be dimensioned.

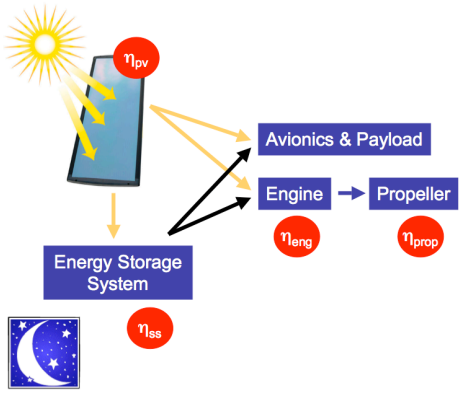

Fig. 3 Block sketch of the UAV energy system

4.1 Energy storage system dimensioning

The amount of energy to be stored will be determined first. Then batteries and a regenerative fuel cell system will be compared.

4.1.1 Amount of energy to be stored

The energy storage system needs to hold all energy required for the flight during the night. The power for the propulsion of the UAV as well as for the avionics and payload needs to be delivered by the storage system throughout the night.

The power required to fly the aircraft P_{fly} can be calculated as

$$P_{fly} = \frac{V}{\eta_{prop} \cdot \eta_{eng}} \cdot q \cdot S_w \left(C_{D,0} + \frac{C_L^2}{\pi \cdot AR_w \cdot e} \right) \tag{1}$$

where V is the flight speed of the UAV $[m/s]$, η_{prop} the propeller efficiency, q the dynamic pressure $[Pa]$, S_w the wing area $[m^2]$, $C_{D,0}$ the zero-lift drag coefficient $[-]$, C_L the lift coefficient $[-]$, AR_w the wing aspect ratio $[-]$ and e the Oswald efficiency factor.

At 20 km and 30 m/s, a power to fly of 6.75 kW is obtained for an engine efficiency η_{eng} of 95 % and a propeller efficiency η_{prop} of 85 %. For the same engine and propeller efficiency at 17 km and 25 m/s, a power of 5.95 kW is needed.

The payload power is given in Table 1 and amounts to 2 kW. The avionics power on the other hand is calculated as 1.2 W per N of avionics mass, which is taken as 3 % of the take-off mass (ref. [7]). This results in a $P_{av,pl}$ of 2.23 kW.

For a night flight of 11 hours, the amount of energy to be stored E_{stor} yields 98.7 kWh.

4.1.2 Energy storage system

Two main options exist for the energy storage system: rechargeable batteries and a fuel cell based system. When reusable batteries are used, the mass of the batteries M_{bat} can be calculated from the following expression:

$$M_{bat} = \frac{E_{stor}}{E_{spec} \cdot (1 - \eta_d)} \tag{2}$$

where E_{spec} is the specific energy or energy density of the battery $[kWh/kg]$ and η_d the discharge rate of the battery, which is defined as:

$$\eta_d = \frac{E_s - E_u}{E_s}$$

where E_s is the amount of energy stored in the battery and E_u the amount of useful energy that can be withdrawn from the battery.

According to ref. [6], Li-ion and Li-Po batteries have an energy density between 100 and 190 Wh/kg. In the Pegasus project, however a prototype Li-S battery is used with an energy density as high as 370 Wh/kg (ref. [3]). Using the later value and an η_d of 0.3 for a total amount of energy required of 98.7 kWh for a night-time operation at summer solstice, a battery mass of almost 380 kg is obtained.

For the fuel cell system an energy density of 500 Wh/kg is adopted for an efficiency of 55% both when working as a fuel cell or as an electrolyser. According to ref. [7], this represents a technology level currently available on the market and comprises the regenerative fuel cell as well as the storage tanks for hydrogen and water. This leads to a fuel cell system weight of 198 kg, or about half of the weight of the battery system.

Only the fuel cell system will thus be retained from here on, as it furthermore represents a technology that is far less mature than batteries and therefore still holds the promise of a possible large weight reduction in the future.

4.2 Solar panel dimensioning

The dimensioning of the solar panels depends on the duration of the night-time operation, which is defined here as the time during which the solar panels do not provide sufficient energy for the payload, avionics and propulsion of the UAV. This depends on its turn on the efficiency of the photovoltaic cells η_{pv} as shown on Figure 4. The figure shows the energy available from the sun at summer-solstice for a latitude of 40°N at approximately 20 km altitude (ref. [5]), the energy available from the solar panels and the energy required for the flight.

Based on references [9] and [16], a value of 20 % is taken for the efficiency of the solar panels which represents a silicium monocrystalline technology. A surface weight of 0.6 kg/m^2 is adopted for this technology (ref. [9]). With this efficiency, approximately 12 hours of the day can be considered as day-time operations (Fig. 4). On top of that, the panels provide sufficient energy for two hours of operation of the payload and the avionics during the night. The total amount of energy to be supplied by the panels is therefore

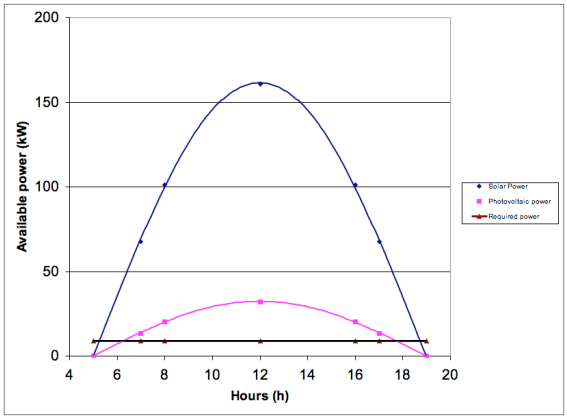

Fig. 4 Available solar energy, available energy from the photovoltaic cells and energy required for the flight

$$E_{PV} = 12 \cdot P_{day} + 11 \cdot \frac{P_{night}}{eta_{FC}} + \left(2 + \frac{10}{\eta_{FC}}\right) \cdot P_{av,pl} \tag{3}$$

where the night-time operation is taken as 11 hrs, with a glide phase of 20 to 17 km of 1 hr, just after sunset. With an electrolyser efficiency η_{FC} of 55%, a total amount of around 290 kWh needs to be stored.

Integration of the curve of the energy available from the fuel cell from Figure 4 shows that the photovoltaic cells can deliver about 2.11 kWh/m^2 at summer-solstice. After adoption of a margin of 5% on the energy provided by the cells a total surface area for the photovoltaic cells of approximately 145 m^2 is found, which leads to a mass of 87 kg for the PV cells.

5 Conceptual design of the HALE UAV

The HALE UAV conceptual design is based on the method laid down in ref. [10] and the mission profile given in Fig. 5. As shown on the figure, the aircraft cycles every day between a cruising altitude of 17 km at night and 20 km at day to reduce the energy stored for the night flight. Below, first the take-off and empty mass of the aircraft will be determined. Once the take-off mass is known, the performance constraints are eval-

uated and the matching plot is set up. In a last subsection, the final wing layout is determined.

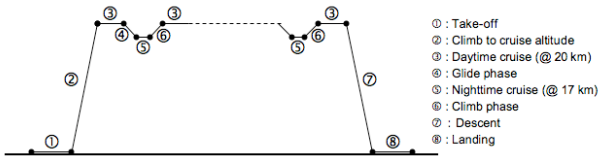

Fig. 5 Mission profile for the HALE UAV

5.1 Determination of the mass of the UAV

Roskam proposes in ref. [10] to use an empirical relationship between the aircraft empty weight and its takeoff weight for the initial sizing calculations which has the following form:

$$\log_{10} W_E = A + B \cdot \log_{10} W_{TO} \tag{4}$$

where coefficients A and B are determined from statistical data. In reference [10], the coefficients are proposed for several aircraft types. Data for HALE UAVs are nonetheless not present. Based on data available from open literature, the coefficients for HALE UAVs are derived, leading to (ref. [1]):

$$A = -0.2927 \qquad B = 1.165$$

For this particular aircraft the take-off weight simply consists out of the empty weight together with payload weight W_{PL} and propulsion and energy storage system weight W_{FC} (no crew and no fuel, as the hydrogen is included in the propulsion and energy storage system weight).

$$W_{TO} = W_E + W_{cargo} = W_E + W_{PL} + W_{FC} \tag{5}$$

The propulsion and energy storage system weight W_{FC} can be expressed as:

$$W_{FC} = \frac{g \cdot t_{night}}{E_{spec} \cdot \eta_{FC}} \cdot \left(P_{fly} + P_{av,pl}\right) \tag{6}$$

The take-off mass in this simplified model thus depends on the values chosen for the wing area S_w, the wing aspect ratio AR_w, the cruise speed V, and the Oswald efficiency factor e and the specific energy and efficiency of the energy storage system E_{spec} and η_{FC} and propulsion system (η_{eng} and η_{prop}). As such, an iteration is required to establish is final value. After iteration a W_{TO} of 6240 N is obtained for a W_E of 3990 N and W_{FC} of 1760 N.

5.2 Performance constraints for the UAV

The required wing area will depend on the performance requirements imposed on the UAV, its drag polar and its take-off weight and is determined from the so-called matching plot. The different requirements considered for the initial sizing of the UAV are briefly reviewed first and the expression that relates the wing and power loading for the requirements is given. Then the drag polar is established before finally all requirements are grouped in the so-called matching plot, leading to the final value of the wing area and propulsive power.

5.2.1 Performance requirements

In the initial sizing step, only three requirements have to be met by the UAV: the stall speed requirement, a maneuvering requirement and a maximum cruise speed requirement. Below, all 3 will be briefly reviewed.

Obviously the UAV has to fly at a speed greater than the stall speed. An upper limit to the wing loading W_{TO}/S_w is therefore imposed as function of the adopted $C_{L,max}$ and the stall speed V_s:

$$\frac{W_{TO}}{S_w} \leq \frac{\rho V_s^2}{2} \cdot C_{L,max} \tag{7}$$

The maximum lift coefficient is set here at 1.2, a reasonably high value seen the low Reynolds numbers at which the wing will operate. In the choice of the stall speed, several factors need to be taken into account. The stall speed itself needs to stay moderate or the propulsive power of the UAV will be excessive. After all, the design cruise speed needs to be higher than the adopted stall speed by a certain margin. This margin is set here to 4 m/s at 20 km and 6 m/s at 17 km. These are namely the speeds of the gusts that can

be encountered at these altitudes. If the aircraft encounters a sudden gust from the tail to the nose, it will just not stall. If the stall speed is chosen too low, on the other hand, the required wing surface will be too high, leading to a heavy UAV as well. At 20 km, a stall speed of 25 m/s is chosen here whereas at 17 km, the stall speed is 20 m/s. This leads to a minimal wing area of approximately 190 m^2 as will be shown later on.

As the UAV will be loitering above a certain area, a maneuvering requirement is also imposed to ensure that the aircraft has a minimal sustained turn rate. Here a turn rate of 20 degrees per second is adopted which results in a load factor n of approximately 1.5. The power required for maneuvering is then determined through:

$$\frac{P}{W_{TO}} = V \cdot \left(\frac{q \cdot C_{D,0}}{W/S_w} + \frac{W}{S_w} \cdot \frac{n^2}{q} \cdot \frac{1}{\pi A R_w e} \right) \quad (8)$$

5.2.2 *Choice of the nominal cruise speed*

As the choice of the cruise speed has a significant influence on the weight and the required power of the UAV, a more detailed study was executed before the final values are fixed. As the cruise phase is a loiter phase the speed leading to a minimal required power is obtained when flying at a lift coefficient of

$$C_L = \sqrt{3 \cdot C_{D,0} \cdot (\pi A R_w e)} \quad (9)$$

As shown by the expression, the optimum lift coefficient only depends on the wing aspect ratio, for a given $C_{D,0}$. This is illustrated on Figure 6. The figure shows the power required to fly at an altitude of 20 km in function of flight speed for different wing aspect ratios.

The figure clearly shows that a strong reduction in the power required can be obtained by an increase in aspect ratio. However, increasing the aspect ratio for a given wing surface area S_w leads to a higher wing span and a lower wing chord. A large wig span leads to a heavier wing as the wing root bending moment increases. The chord reduction is however even more important as it leads to low Reynolds numbers for the wing, which might reduce the maximum lift coefficient

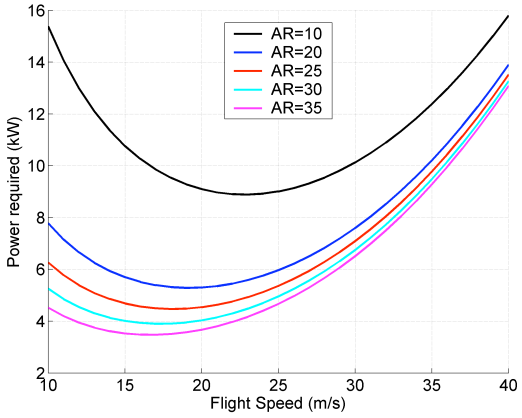

Fig. 6 The power required at 20 km altitude for different AR_w

and also increase the zero lift drag of the wing. Às a compromise, a wing aspect ratio of about 30 is adopted here, which is in line with values from Global Hawk, Helios and other HALE UAV studies (ref. [2], [7] and [8]).

Figure 7 gives the power required for the aspect ratio of 30 at altitudes of 17 and 20 km. Based on this diagram, the nominal cruise speeds will be fixed. At 20 km, it is shown that the required power increases rapidly for cruise speeds higher than 25 m/s. To keep a reasonable margin with respect to the stall speed, a value of 30 m/s is adopted, resulting in a power required of approximately 5.5 kW and a lift coefficient of 0.83. At 17 km, the cruise speed is on the other hand set to 25 m/s resulting in a power required around 6.0 kW at a C_L of 0.81. As 6.75 kW was used in the sizing of the solar panels, a small additional 'reserve' energy of approximately 8.5 kWh is available for emergency or when excessive maneuvering is required. A part of this energy will be used in the daily morning climb from 17 km up to 20 km altitude.

5.2.3 *Drag polar*

Following the guidelines from ref. [10], a parabolic drag polar is adopted in this work:

$$C_D = C_{D,0} + \frac{C_L^2}{\pi \cdot AR_w \cdot e} \quad (10)$$

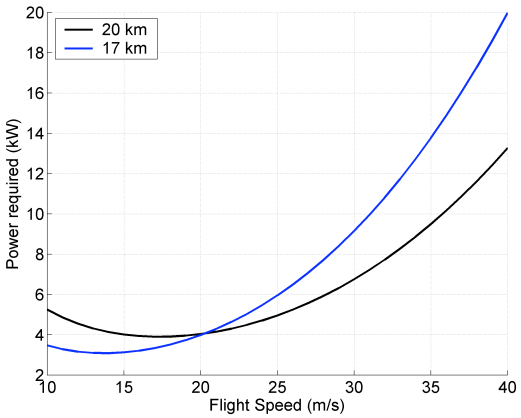

Fig. 7 The power required at 17 and 20 km for $AR_w = 30$

so only the Oswald efficiency factor e and the zero-lift drag coefficient $C_{D,0}$ need to be estimated. As no correlations were found in literature for this specific application, the zero-lift coefficient was derived from performance data available for other UAVs of the same type (ref. [1]) and a value of 0.018 was found.

The Oswald efficiency factor is on the other hand determined from reference [12]. As shown on Figure 2 (ref. [12]), the span efficiency factor depends on the vertical separation between the wings and the height of the winglets. Seen the high aspect ratio of the wing (30) and the important wing area (190 m^2), a span of around 75 m is namely obtained. The height to span of the wing is thus limited to 0.17, the lowest value indicated on the figure. The winglet height is limited to 60 % of the vertical separation of the wing, yielding an Oswald efficiency factor of 1.2.

The drag polar is then given by:

$$C_D = 0.018 + 0.0088 \cdot C_L^2$$

5.2.4 Matching plot

As all necessary data has been obtained, the matching plot can be drawn. It is given on Figure 8. The full lines on the figure represent the requirements at 20 km altitude while the dashed lines indicate values for 17 km altitude. The black dot gives the design point for the UAV. For 20 km altitude, a maneuver speed of 30 m/s was adopted whereas the maximum cruise speed was set at 37.5 m/s. For 17 km, these speeds are 25 respectively 30 m/s. The stall speeds were taken as 25 and 20 m/s for 20 respectively 17 km altitude as indicated before. As shown on the figure,

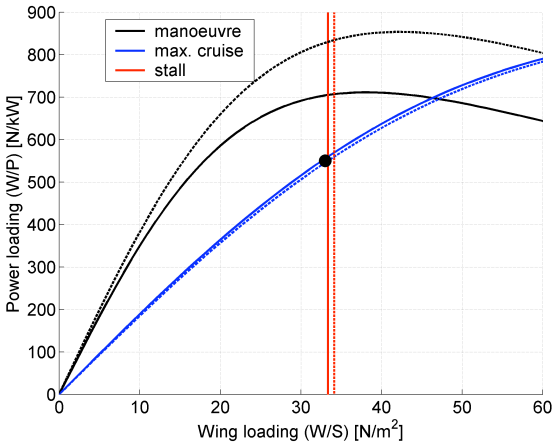

Fig. 8 The matching plot for the HALE UAV

the selected stall speeds give a similar wing area for both altitudes. The power required is clearly set by the maximum cruise speed requirement. The final design point is given by:

$$\left(\frac{W_{TO}}{S_w}\right) = 33\frac{N}{m^2} \qquad \left(\frac{P}{W_{TO}}\right) = 575\frac{N}{m^2}$$

With the take-off weight of the aircraft determined previously, this leads to a wing surface area of 189 m^2 and a take-off power of 10.85 kW.

The 10.85 kW power will be provided by 8 electric motors with a maximum power of around 1.6 kW, weighing approximately 5.2 kg each. Each motor drives a 2 bladed propeller which has a blade power loading of about 32 kW/m^2 and a diameter of approximately 18 cm (ref. [1]).

5.3 Wing design

As a relatively ambitious maximum lift coefficient was set to determine the stall speed and as the wing design is critical to the success of the HALE UAV under consideration, a preliminary assessment of the airfoil selection and wing planform choice is made below.

5.3.1 *Wing airfoil*

The airfoil chosen for this HALE UAV is the DAE 21, which has also been used on SHAMPO (ref. [7]). The profile has a high maximum lift coefficient and has been optimized for a Reynolds number of 375000. The maximum thickness over chord ratio of the profile is 11.78%. The profile lift and drag characteristics have been assessed with XFOIL and the results are given on Figure 9 for various Reynolds numbers.

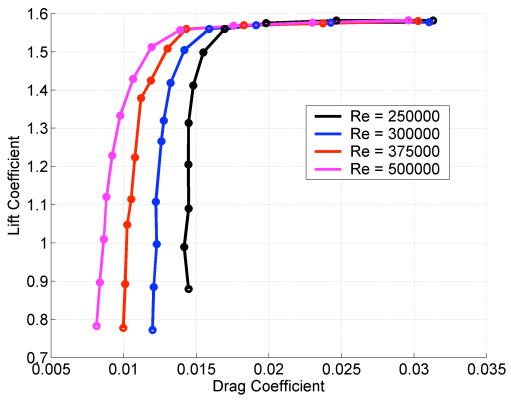

Fig. 9 The lift and drag coefficients for DAE21

5.3.2 *Wing planform*

The selection of the joined-wing planform is mainly set by two criteria: the minimum allowable Reynolds number which will set the surface distribution between the lower and the upper wing and the shade of the top wing on the low wing which determines the wing sweep.

As the maximum chord for both sections of the joined-wing is obtained by allocating half of the total wing area to each section, the front and aft section of the wing will consist of half the total wing area or 94.5 m^2. As the overall wing aspect ratio and thus the wing span have been fixed to keep the induced drag low, all geometric characteristics have been determined. The wing taper ratio is namely selected as 1 in order not to decrease the Reynolds number even further. After all, with the current design, a Reynolds number of approximately 325000 is obtained at 20 km, whereas at 17 km the Reynolds number of the wing lies around 375000. The chord of both sections of the wing is 1.255 m.

The wing sweep is a compromise between wing weight, increasing with increasing sweep, and the amount of sunlight blocked by the upper wing. If no sweep is used, the upper wing will block the direct sunlight for the lower wing during a considerable portion of the day and a significant amount of energy will be lost for the solar panels of the lower wing. Knowing the evolution of the sun around the hemisphere, the amount of energy lost can be determined as a function of the wing sweep (ref. [1]). Selecting a sweep angle of the front wing Λ_F of 15° and of the aft wing Λ_A of 10° gives a reduced electricity production of about 1.9 hours during the day (in the early morning and late evening). It is therefore considered a good compromise between wing structural weight and energy lost. The amount of energy lost is furthermore minimized by covering almost the complete surface of the aft upper wing with solar panels. As only 135 m^2 of solar panels was required, the front wing only has 45 m^2 of solar panels.

With the planform and airfoil fixed, the 3D maximum lift coefficient can be determined. Using the methods from reference [10], a value slightly higher than 1.2 is obtained. The previously selected value for the maximum lift coefficient has thus been obtained.

5.4 Vertical tail design

As the joined wing requires no additional horizontal tail, only the vertical tail needs to be sized. Its surface is determined using the classical tail volume coefficient approach (ref. [10]). The volume coefficient is taken as 0.4 and the taper ratio of the tail is set to 0.1 as this yields a tip chord equal to the wing chord. The tail height is set by the vertical separation of the wing (13.03 m) so all parameters are fixed. The vertical tail surface area is 83 m^2.

6 Conclusions and future work

As shown, the adoption of a joined-wing configuration for a HALE UAV leads to several inter-

esting synergies. Not only will the Oswald efficiency factor be increased to values in the order of 1.2, the wing structural weight will be reduced too, seen the stiffness added by closing the 'wing box'. As the low power requirement, a key driver for HALE UAVs, leads to low cruise speeds and high wing surfaces, the joined-wing potentially offers a significant benefit for this particular application.

In a next step, a more detailed assessment of the aerodynamic and structural characteristics of the wing will be made. The refined results will then be used to iterate on the overall design of the UAV. A preliminary view of the HALE UAV is given in Figure 10.

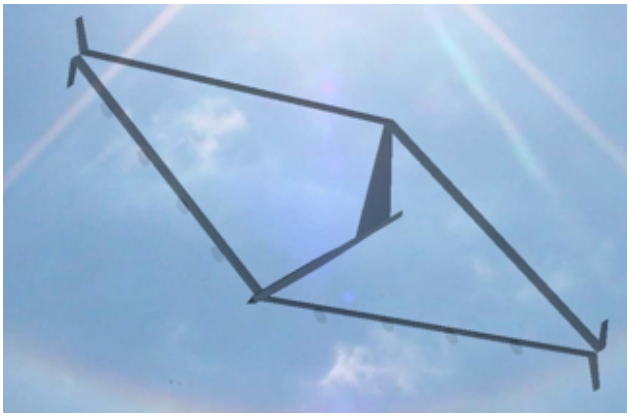

Fig. 10 A preliminary view of the joined-wing HALE UAV

References

[1] M. Coatanéa, *Avant-Projet d'un drone haute altitude*, Mémoire de fin d'études, Université Libre de Bruxelles, 2007.

[2] F. Dewispelaere, The first Pegasus technology demonstrator for remote sensing applicaitons, *2nd International workshop on the future of remote sensing – Tutorial*, VITO, Mol, Belgium, 2006.

[3] J. Everaerts, Background of the Pegasus project, *2nd International workshop on the future of remote sensing – Tutorial*, VITO, Mol, Belgium, 2006.

[4] L.R. Jenkinson and J.F.. Marchman, *Aircraft Design Projects for Engineering Students, Illustrated*, AIAA Education Series, 2003.

[5] G.A. Khoury and J.D. Gilett, *Airship Technology*, Cambridge University Press, 1999.

[6] J. Robert and J. Alzieu, *Accumulateurs - Considérations théoriques*, Techniques de l'ingénieur, *www.techniques-ingenieur.fr*, 2007.

[7] G. Romeo and G. Frulla, HELIPLAT : Aerodynamic and Structural Analysis of HAVE Solar Powered Platform, *AIAA 1st Technical Conference and Workshop on Unmanned Aerospace Vehicles*, Portsmouth, Virginia, 2002, AIAA-2002-3504.

[8] G. Romeo, G. Frulla, E. Cestino and F. Borello, SHAMPO : Solar HALE aircraft for multi payload and operations, *Aeronautica Missili e Spazio*, Vol. 85, 2006.

[9] G. Romeo, High Altitude Very Long Endurance Solar Powered UAV for Earth Observation and Border Patrol Applications, *RISE 2006*, Royal Military Academy of Belgium, Brussels, 2006.

[10] J. Roskam, *Airplane Design Parts I-VIII*, DARcorporation, 1997.

[11] P. Van Blyenburgh, *Unmanned Aircraft Systems: The global perspective*, Conférence, Université Libre de Bruxelles, 2007.

[12] J. Wolkovitch, The joined wing: An overview, *AIAA 23rd Aerospace Sciences Meeting*, Reno, Nevada, USA, 1985, AIAA-85-0274.

[13] The World Wide Web, *USE HAAS: Study on High Altitude Aircrafts and Airships (HAAS), Deployed for Specific Aeronautical and Space Applications, Stategic Agenda Vol 3*, http://www.usehaas.org, 2007.

[14] The World Wide Web, *http://www.sun-h2.be*, 2008.

[15] The World Wide Web, *http://www.hapcos.org*, 2008.

[16] The World Wide Web, *http://en.wikipedia.org/wiki/SolarCell*, 2007.